

1 Cropping pattern switching induces disturbances in spatiotemporal greenhouse gas emissions and water demand

2 Yihe Tang ^{1,2,3}, Shikun Sun ^{1,2,3*}, Fei Mo ⁴, Thomas W Crowther ⁵, Yali Yin ^{1,2,3}, Jinfeng Zhao ^{1,2,3}, Yubao Wang ^{1,2,3}, Pute

3 Wu ^{1,2,3}

⁴ ¹ Key Laboratory of Agricultural Soil and Water Engineering in Arid and Semiarid Areas, Ministry of Education,

5 Northwest A&F University, Yangling 712100, Shaanxi, China

² Institute of Water Saving Agriculture in Arid regions of China, Northwest A&F University, Yangling 712100, Shaanxi, China

³ National Engineering Research Center for Water Saving Irrigation at Yangling, Yangling 712100, Shaanxi, China

⁹ ⁴College of Agronomy, Northwest A&F University, Yangling, 712100, Shaanxi, China

¹⁰ ⁵ Institute of Integrative Biology, ETH Zürich, 8092, Zürich, Switzerland

11 *Corresponding author: Sun SK(ksun@nwafu.edu.cn)

12 College of Water Resources and Architectural Engineering, Northwest A&F University, Yangling 712100, P. R. China
13

14 **Abstract**

15 Balancing food security with sustainable agriculture production poses a significant contemporary challenge. Adjusting
16 cropping patterns is a potent measure, yet the dual impact on environments and spatial variations resulting from this
17 transformation remains unclear. Utilizing process-based crop models and high-precision crop cropping pattern maps, this
18 study evaluated the water demand and greenhouse gas (GHG) emissions of major grain in China. This aimed to determine
19 regional responses to changes in cropping patterns. The shift in China's cropping patterns from wheat to rice and corn
20 increased agricultural soil GHG emissions and water demand, peaking in 2015 at 898.52 TgCO₂e and 541.92 Gm³.
21 Variability in GHG emissions and water demand is observed among different grain and regions. Spatial disparities are
22 influenced by crop types and scales, while intra-regional differences stem from the distribution of different crops. These
23 results guide the redirection of grain production towards patterns with minimal environmental impact, and are crucial for
24 achieving a sustainable agricultural production structure.

25 **Keywords:** Cropping pattern, Greenhouse gas, Water demand, Grain, DNDC

26

27 **Main**

28 China's agricultural productivity has grown rapidly over the past few decades, with grain production increasing by
29 107% since 1990¹. The high rate of agricultural development has been accompanied by an increased burden on resources
30 and the environment. The emission of greenhouse gases (GHGs) from agricultural production is one of the significant
31 factors causing climate change. The global food production system emits approximately 16.5 Gt CO₂ eq·yr⁻¹ of GHGs,
32 accounting for 31% of the total anthropogenic emissions², with the agricultural sector is the main source of CH₄ and N₂O
33 emissions, contributing to nearly 50% of CH₄ emissions and 75% of N₂O emissions³. Additionally, agricultural
34 production is the largest consumer of freshwater resources, accounting for 70% of the world's total water resources⁴. The
35 growing population and demand for grains have increased the demand for water resources and the pressure on the
36 environment⁵. Achieving water-saving and emission reduction in agriculture while ensuring food security is a challenge
37 facing the agricultural sector.

38 Based on the pressures mentioned above, the agricultural sector has implemented several measures to improve the
39 sustainability of agricultural production⁶⁻⁸. These measures include adopting water-saving irrigation techniques and
40 applying fertilizer quotas. However, it is important to note that these strategies assume crops are already cultivated in the
41 optimal area¹. Cropping patterns reflect the types and scales of crop planting in a certain region^{9,10}. Cropping patterns
42 are influenced by various factors, such as climate, regional planting conditions, government policies, and economic
43 returns^{11,12}. Adjusting cropping patterns is a key solution for achieving sustainable agricultural management, effectively
44 complementing field management practices. The Chinese government, as highlighted in multiple documents, achieves
45 sustainable agricultural development through cropping pattern adjustments. To ensure food security while considering
46 local conditions and the ecological environment, three major zones have been established: optimal development zones,
47 moderate development zones, and conservation development zones. Therefore, assessing the impact of different crops on
48 GHG emissions and water demand, as well as the combined effects of diverse cropping patterns, plays a pivotal role in
49 achieving sustainable agricultural development across various regions in China.

50 There are notable inter-regional and inter-crop disparities in crop GHG emissions and water requirements. These
51 variations primarily drive the impact of changes in cropping patterns on regional GHG emissions and water requirements
52¹³⁻¹⁵. Rice, wheat, and corn show significant differences in nitrogen use efficiency, which resulted in the difference of
53 their fertilization management practices, such as fertilization timing, amount, and frequency¹⁶. In addition, the
54 physiological differences among crops, including root depth, root length density, root hairs, and nitrogen transport protein

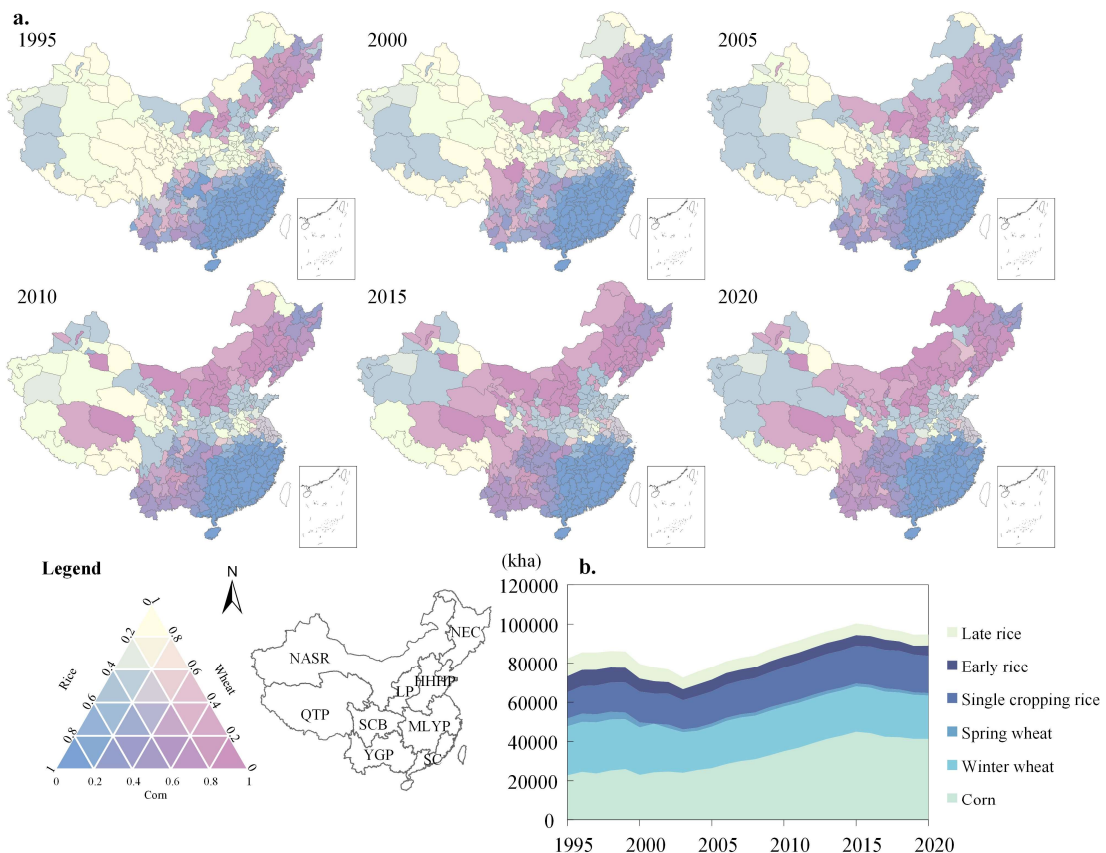
systems, play an important role in affecting the nitrogen absorption efficiency for renewable energy ¹⁷, which is also a significant reason for the different nitrogen fertilizer requirements for crops. As the evolution of cropping patterns inevitably leads to different nitrogen fertilizer consumption in the entire system, the nitrogen input amount is one of the most critical factors affecting GHG emissions ^{18,19}. The physiological differences among crops also lead to different water demand differences. Rice and wheat are C3 crops, while corn is a C4 crop. Compared with C3 crops, C4 crops absorb more carbon and lose less water through crop transpiration ²⁰. Climate, topography, and regional environments result in different sowing dates for rice, wheat, and corn, which is an important factor affecting crop water demand ²¹.

This study quantified and evaluated the GHG emissions and water requirements of China's major grain crops from 1995 to 2020, while examining the spatiotemporal variations in response to disturbances caused by different cropping patterns. There are two keys: 1. Assessing the influence of cultivation scale changes on overall GHG emissions and water demand. 2. Examining the effect of regional crop cultivation variations on GHG emission intensity and water demand intensity. We concentrated on three key grain crops – rice, wheat, and corn – which collectively contribute to 91% of China's major grain crop production and occupy 81% of the total planted area. Furthermore, these crops exhibit widespread distribution across various provinces in China. The DNDC model served as the primary quantitative tool in this study. We validated its applicability to various crops within each region using empirical data from 31 sets of peer-reviewed publications at the point level. Additionally, we developed a set of municipal-scale crop parameters tailored to the specific conditions of China's municipalities. The study sought to comprehensively evaluate the impact of changes in cropping patterns on agricultural water demand and GHG emissions, providing a scientific basis for water conservation and emissions reduction in China's agriculture.

74

75 **Results**76 **Grain cultivation scale's influence on GHG emissions and crop water demand trends**

77 The scale of grain cultivation affects GHG emissions and total crop water demand. During the study period, the scale
 78 of grain cultivation in China showed a fluctuating upward trend, with four distinct stages of change (Fig. 1b,
 79 Supplementary Results). In 2015, China's grain cultivation area reached a maximum value of 102.33 Mha. Along with
 80 the changes in grain scale, China's grain GHG emissions and water demand also went through a phase of increasing and
 81 then decreasing, reaching a peak in 2015 at 898.52 TgCO₂e, and 541.92 Gm³, respectively.



82
 83 Fig. 1 Cropping pattern of major grain. (a.) Proportions of major grain in each city area, using a ternary graph as legend,
 84 where colors closer to blue indicate higher proportions of rice, closer to yellow indicate higher proportions of wheat,
 85 and closer to pink indicate higher proportions of corn. (b.) Stacked area graph showing changes in china's major grain
 86 from 1995 to 2020.

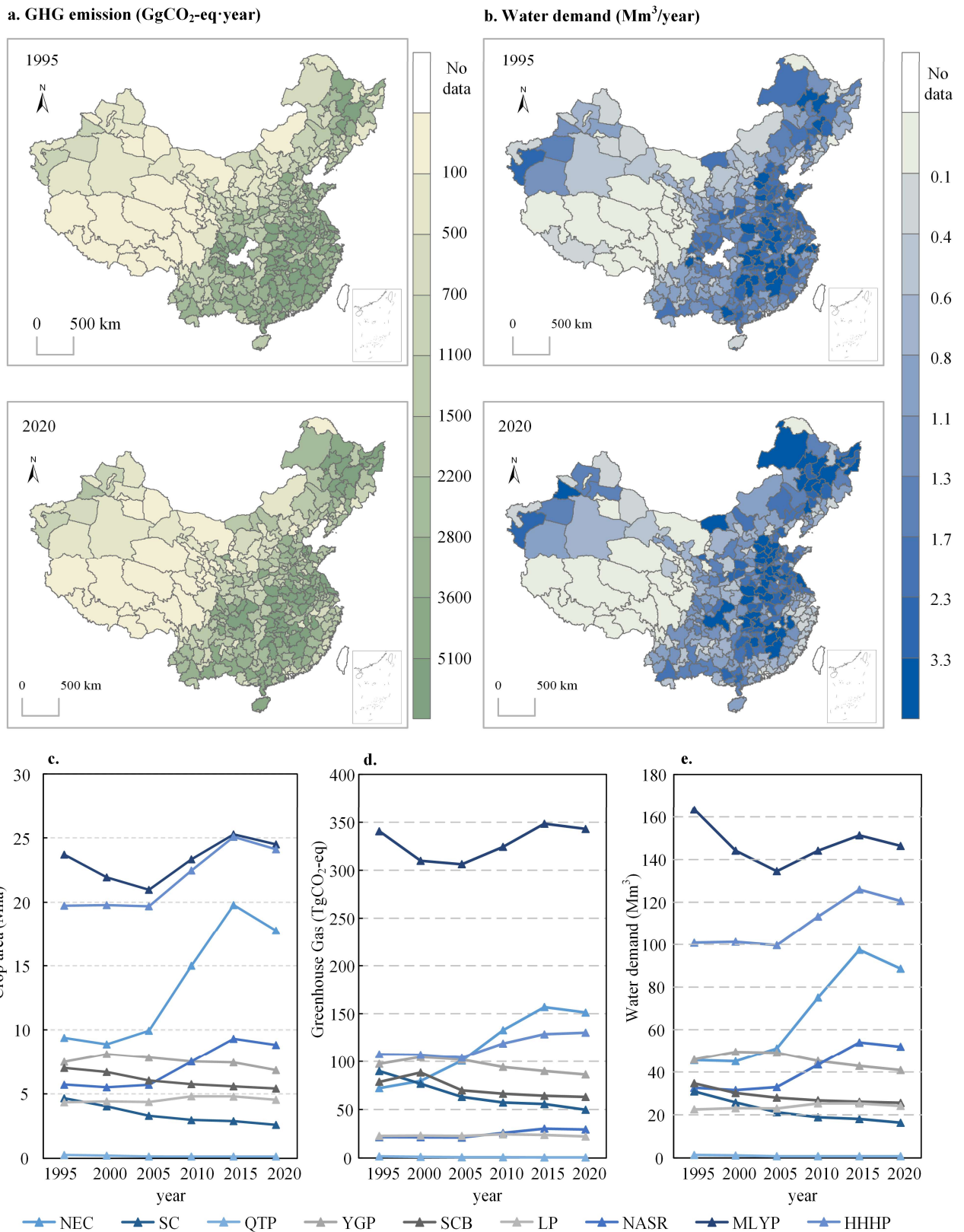
87 The study analyzed the spatial and temporal distribution patterns and spatial heterogeneity of total emissions and
 88 total water demand of grain crops in China from 1995 to 2020, using the city as the basic unit. (Fig. 2a, b; Fig. S1; Fig.
 89 S2).

90 Substantial disparities in both the total quantity and trends of GHG emissions across different regions are evident
 91 (Fig. 2a, d). The Middle and Lower Yangtze Plain (MLYP), a key grain-producing region in China, consistently

92 maintained a higher level of total emissions, accounting for 18.53% of the total emissions in 2015. Reflecting these overall
93 high emission levels, MLYP exhibited elevated levels of CO₂, N₂O, and CH₄ emissions compared to other regions. This
94 can be attributed to the relatively fewer constraints on crop cultivation in the MLYP region, making it conducive to the
95 growth of most grain crops. The extensive cultivation of crops such as corn, wheat, and rice, with a significant proportion
96 dedicated to rice cultivation, notably contributes to higher CH₄ emissions in MLYP compared to other regions (Fig. S3c).
97 Despite the expanded grain cultivation in the Northeast China Plain (NEC) during the study period, which reduced the
98 CO₂ and N₂O emission shares of MLYP, CH₄ emissions in NEC peaked in 2015 at 6.31 TgC/yr due to increased cultivation
99 area. This peak is attributed to NEC not being a primary region for rice cultivation, especially for early and late-season
100 rice varieties, which were not grown in the region. The diversity of grain types cultivated is a key factor influencing the
101 overall quantity of GHG emissions (Xiao et al., 2022).

102 The Huang-Huai-Hai Plain region (HHHP), being the largest rainfed crop cultivation area in China, exhibited CO₂
103 and N₂O emissions second only to MLYP. Moreover, due to the expansion of rainfed crop cultivation areas, these
104 emissions showed an increasing trend. Between 1995 and 2015, the CO₂ and N₂O emissions from NEC demonstrated a
105 continuous upward trend, surpassing HHHP to become the second-largest emission region in China. The primary cause
106 of this shift is the sustained expansion of corn and single cropping rice cultivation areas in the NEC region.

107 In contrast, the Northern Arid and Semi-Arid Region (NASR) contributes a relatively modest annual average share
108 of 3.30% to GHG emissions, with minimal discernible annual fluctuations. The regional variations in GHG emissions
109 align closely with the overall changes in grain crop cultivation scale across China, particularly evident in the Southeast
110 and Northeast regions. As the cultivation area expanded, the total emissions from the Northeast region surged from the
111 fifth position nationally to the second, underscoring the profound impact of changes in cultivation scale on regional
112 emission dynamics.



113

114 Fig. 2 GHG emission of China's major grain. (a.) Spatiotemporal distribution of GHG emission equivalents in various
 115 cities; (b.) Emission levels of three agricultural sources of GHGs in China's major agricultural areas. Regional line
 116 graphs depicting changes in a. crop area, b. total GHG emissions, and c. crop water demand for each agricultural region
 117 in China over the study period.

118 Aligned with the trends in total GHG emissions, China's overall grain water demand exhibits a three-phase variation,
119 driven predominantly by the MLYP, HHHP, and NEC regions. In comparison to GHG emissions, the trends in water
120 demand across regions demonstrate a higher degree of concordance with changes in crop cultivation areas (Fig. 2c, e).
121 MLYP consistently maintains the highest water demand, attributable to its extensive cultivation scale. While HHHP's
122 grain cultivation area is similar to MLYP, the water demand is considerably lower due to the different crop types planted.
123 HHHP predominantly cultivates corn and winter wheat, resulting in lower water demand compared to MLYP's cultivation
124 of single cropping rice. Moreover, the correlation between crop water demand, GHG emissions, and cultivation scale is
125 not strictly positive; regions with larger cultivation scales do not necessarily exhibit higher GHG emissions or water
126 demand. This phenomenon becomes particularly evident when comparing regions with similar cultivation scales, as
127 observed in 2000 for NEC and the Yun-Gui Plateau (YGP). The primary cause of this phenomenon lies in the
128 physiological differences among different grains, implying distinct GHG emission intensities and water demand for
129 different crops. Simultaneously, the physiological characteristics of the same crop may significantly differ when cultivated
130 in different regions.

131 **Spatial and crop disparities in GHG emissions and water demand intensity**

132 To alter cropping patterns significantly, adjusting the crop composition is crucial. Regional variations in GHG
133 emission intensity during this transition primarily stem from variations in emissions and water demand across different
134 crops. To assess emission disparities across regions, this study employed heat maps illustrating GHG emission intensity
135 and crop water demand intensity (i.e., Water Demand per unit area, WDP) for various crops (Fig. 3; Fig. 4b; Fig.S5).

136 High emission intensity regions align spatially with areas of elevated temperature and precipitation (Fig. S4),
137 mirroring the broader regions exhibiting high total GHG emissions. Notably, emission hotspots vary among crops. Maize
138 emissions peak in South China (SC) at an average intensity of 8166.69 kgCO₂e/ha, while spring wheat's hotspot is
139 primarily in NEC, with an intensity of 13516.86 kgCO₂e/ha. Emission hotspots for winter wheat show minimal spatial
140 differences, except in QTP and NASR where intensity ranges from 5000 to 7000 kgCO₂e/ha. Rice, a significant emitter
141 of CO₂, N₂O, and CH₄, surpasses other dryland crops in emission intensity, averaging 17,835.44 kgCO₂e/ha. Emission
142 hotspots for early and late rice align with crop distribution, concentrated mainly in the YGP.

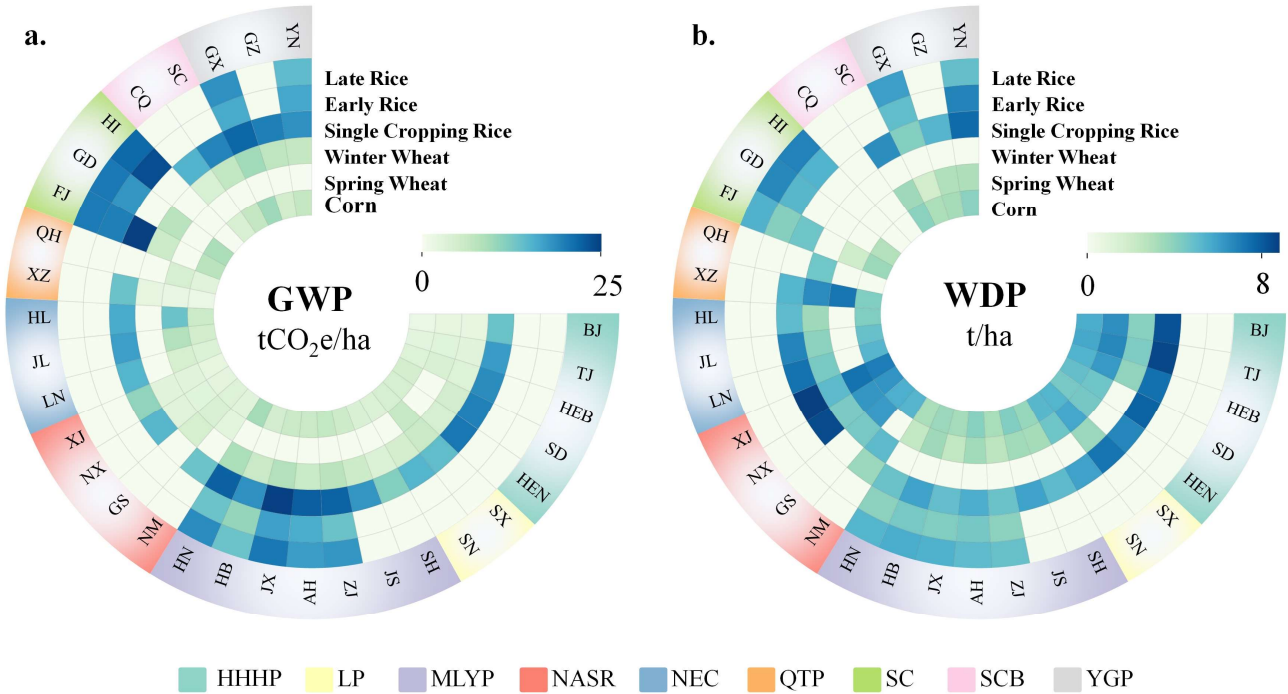
143 This paper generated maps illustrating the spatial and temporal shifts in the proportions of maize, rice, and wheat—
144 the three primary grain—across various cities (Fig. 1a). Since 1995, cities in northern China, encompassing the Northeast
145 and Northwest, have witnessed a gradual transition from wheat, previously the predominant crop (>50% of planted area),

146 to an increasing prevalence of maize and rice. The number of cities where maize serves as the main crop has surged from
147 53 in 1995 to 133 in 2020, marking a notable 150.94% increase. This transformation has largely displaced wheat as the
148 primary crop in most provinces.

149 Rice has maintained its dominant status in the number of cities, showing no significant spatial or temporal trend,
150 owing to its unique growing conditions. Substantial variations in primary crops exist within agricultural zones. Cities
151 predominantly cultivating wheat are concentrated in the northwestern and central regions of China. Corn-dominated areas
152 are primarily found in the northeastern, northern, and southwestern regions, with a discernible expansion trend toward
153 the northwestern and central regions. Rice-dominated regions are concentrated in the southeast and northwest, with
154 double-season rice prevailing in the southwest and single cropping rice dominating the rest of the country.

155 Both wheat and maize, categorized as dryland crops, share similar emission characteristics. Transitioning from wheat
156 to maize has negligible impacts on overall emission intensity. In contrast, the emission dynamics of rice, especially single
157 cropping rice, diverge significantly from those of dryland crops. In provinces like HL, SH, and GZ, where the conversion
158 of dryland crops to rice reached 22.04%, 17.03%, and 12.98%, respectively, CH_4 emission intensity saw substantial
159 increases of 1.5%, 34.5%, and 39.9%, respectively. Notably, this relationship is not linearly correlated. XZ province
160 exhibited the highest CH_4 emission intensity surge by 60%, despite not having the largest increase in rice cultivation area.

161 The disparity in CH_4 emission intensity among provinces is further accentuated by the specific environmental
162 demands of rice cultivation. A horizontal comparison of inter-annual changes in each province reveals a decreasing trend
163 in CO_2 and N_2O emission intensities, while CH_4 emission intensity exhibits a fluctuating upward trend. The main driver
164 for this trend is the shift from dry cultivation to rice as the primary crop.



165

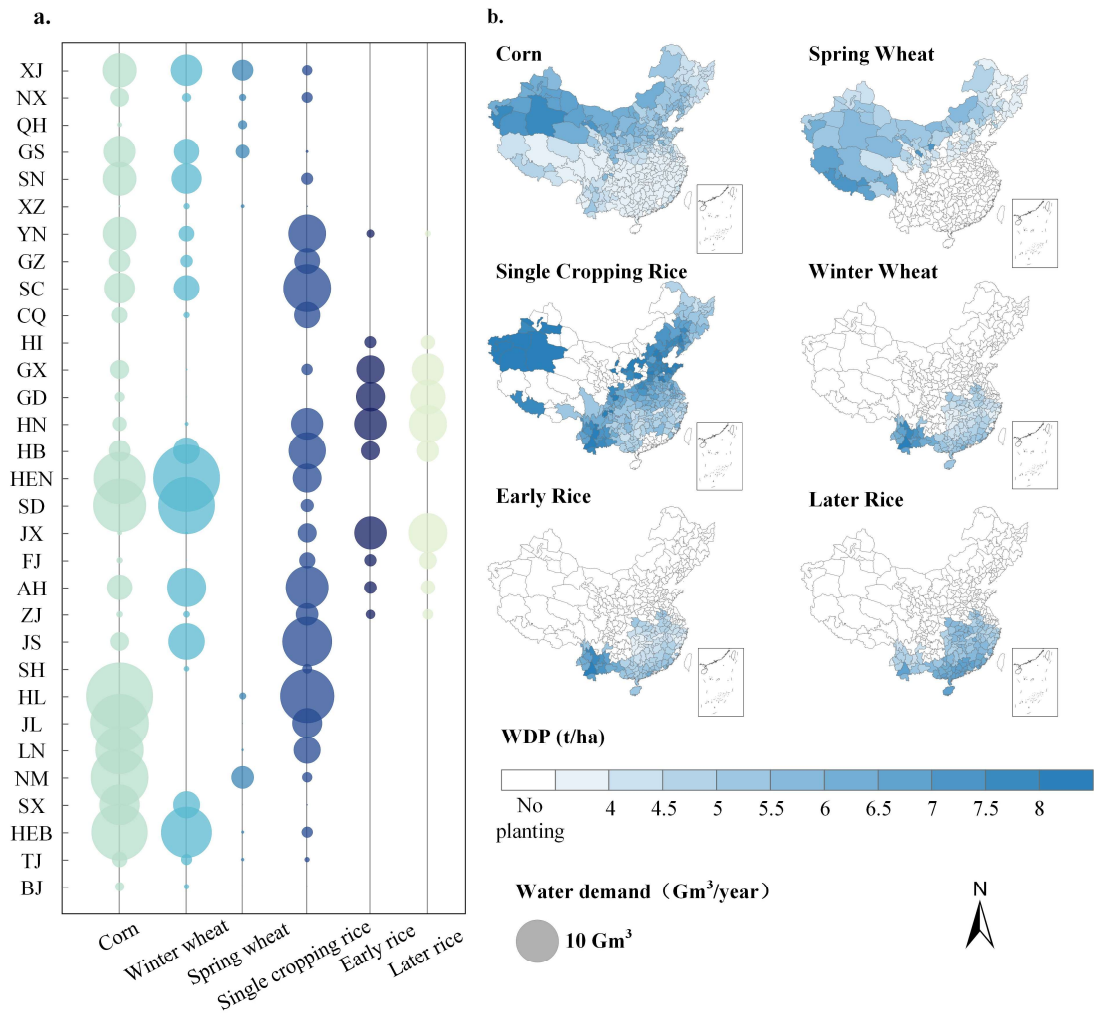
166 Fig. 3 Heat Map of provincial GHG emissions (a.) and water demand (b.) per unit area. The colour of the outermost
167 circle represents the agricultural region to which the province belongs.

168

169 Conversely, the water demand per unit area (WDP) for crops exhibits a contrasting pattern to the spatial distribution
170 of GHG emission intensity. Regional climate emerges as the primary factor influencing variations in WDP for the same
171 crop across different regions. The regions with higher WDP align with areas characterized by low temperature and low
172 precipitation (Fig. 4b; Fig.S4).

173

174 Maize and winter wheat in NASR, monoculture rice in HHHP, spring wheat in QTP, and early and late rice in SC
175 generally demonstrate elevated WDP values. Disparities in crop types directly impact crop fertility and coefficients,
176 contributing to variations in WDP values among crops. Single cropping rice holds the highest national average WDP at
177 4.87 t/ha, while spring wheat exhibits the lowest national average WDP at 3.11 t/ha. Considering the cumulative impact
178 of multiple crops, NASR registers the highest WDP at 5.81 t/ha, attributed to its lower average annual precipitation.



177

178 Fig. 4 Water demand for major grain in China. (a.) Bubble map of total water demand in 2015 for each provincial
 179 administrative region in China, with crops differentiated by different colours; (b.) ET_c for each municipal administrative
 180 region in China in 2015, with white indicating that the crop was not grown in that region

181 The water demand per unit area in JS province consistently exceeded that of other provinces throughout all years
 182 (Fig. 4). This disparity primarily results from over 98.23% of JS province being dedicated to rice cultivation, a notably
 183 water-intensive grain. Similarly, GX, HN, and FJ, with cropping patterns akin to JX, also exhibit elevated water demand
 184 per unit area. Overall, 21 provinces displayed a decreasing trend in water demand per unit area (Fig. S6), with ZJ
 185 experiencing the most fluctuation—from 804.25 mm/year in 1995 to 541.20 mm/year in 2020, with a 48.61% decrease.

186 Contrastingly, some provinces witnessed an increase in crop water demand per unit area, with NX province leading
 187 in this aspect—rising from 567.45 mm/year in 1995 to 677.95 mm/year in 2020, a 19.47% increase. Notably, NX's shift
 188 from wheat to maize dominated its cropping pattern during the study period, with no significant fluctuation in rice
 189 cultivation area. Given the substantial variation in water requirements among crops, altering the cropping pattern can
 190 significantly impact regional water needs. A shift towards high water-consuming crops, like single cropping rice and

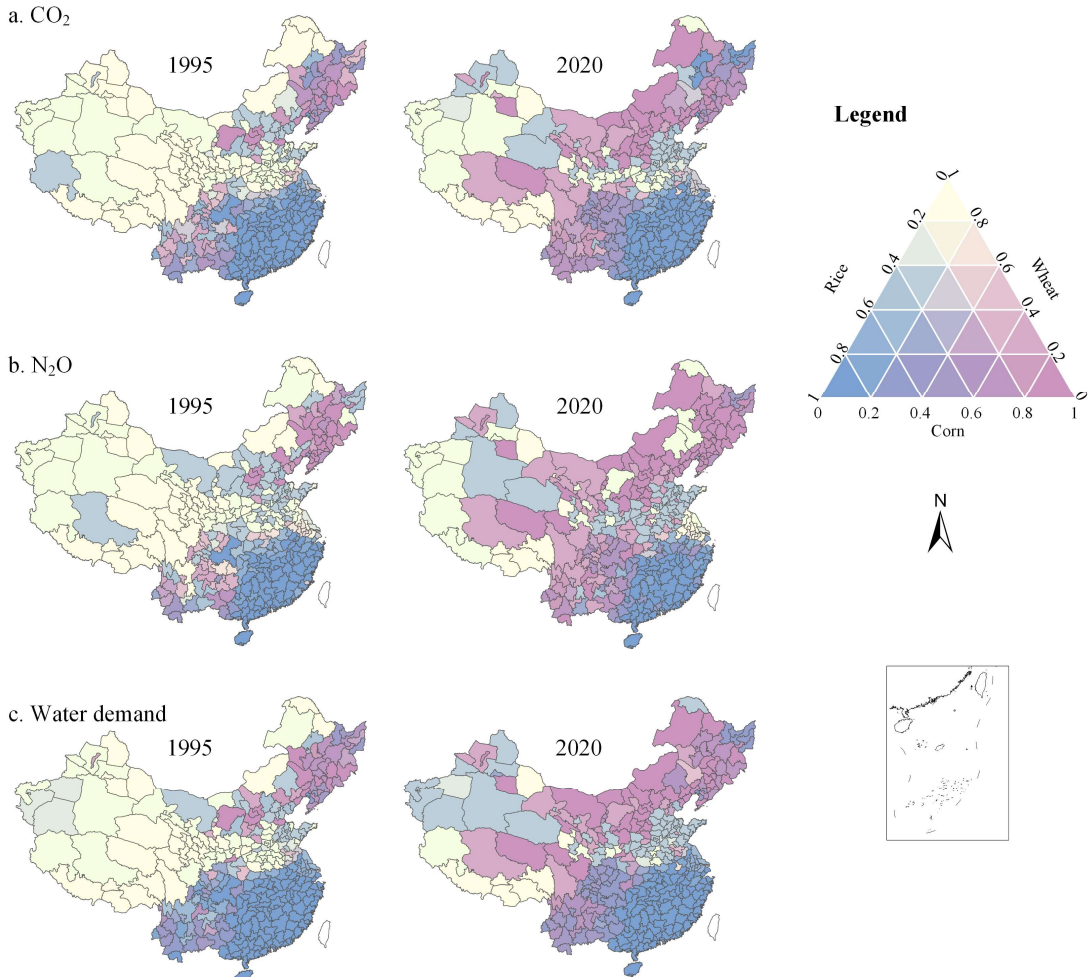
191 maize, may markedly increase average WDP in the region, contingent on the proportion of such crops. Given the dual
192 challenges of high emissions and water demand, judicious adjustments to regional single cropping rice cultivation can
193 effectively advance agricultural water conservation and emission reduction.

194 **Perturbation of agricultural GHG emissions and water demand by cropping patterns**

195 To evaluate variations in GHG emissions from the three primary grain across diverse regions, accounting for
196 discrepancies in cropping patterns and cultivation scale, we computed CO₂ and N₂O emissions individually for each crop.
197 To ensure uniformity, spring and winter wheat were collectively classified as wheat, while all three varieties of rice were
198 treated as a single category. It is important to highlight that CH₄ emissions, mainly originating from rice cultivation, were
199 omitted from this analysis.

200 As depicted in Fig. 5a, the contribution of major grains to CO₂ emissions in China underwent substantial changes
201 from 1995 to 2020. Notably, regions previously dominated by wheat witnessed a shift towards areas predominantly
202 cultivating rice and maize. This observed trend aligns closely with concurrent alterations in cropping patterns over the
203 same period.

204 Over the study period, the primary source of CO₂ emissions in the NEC shifted from rice in 1995 to maize crops.
205 Maize dominance surpassed that of rice, while wheat's dominance experienced a slight decline. Similarly, YGP exhibited
206 a trend consistent with NEC, with a more pronounced increase in areas dominated by maize. In NASR, CO₂ emissions
207 were initially dominated by wheat, gradually transitioning to rice and maize crops. Contrastingly, MLYP and SC saw no
208 significant shift in the crops dominating CO₂ emissions, with rice remaining the predominant contributor throughout the
209 study period, particularly in SC where it constituted the largest share of municipal emissions.



210
 211 Fig. 5 Contribution of major grain to (a.) CO₂ (b.) N₂O emissions c. water demand in 1995 and 2020. The legend is a
 212 ternary graph showing the contribution of each crop to the emissions in the region, the closer the colour to blue the
 213 greater the contribution of rice, the closer the colour to yellow the greater the contribution of wheat and the closer the
 214 colour to pink the greater the contribution of corn; other years see FigS7-FigS9.

215 The contribution of major grain to N₂O emissions exhibits noteworthy inter-annual variations. In the NEC, maize
 216 has emerged as the primary contributor to N₂O emissions, with an increasing number of municipalities dominated by
 217 maize emissions and a corresponding decrease in those dominated by rice emissions. Similarly, in YGP, the dominance
 218 of rice emissions has gradually given way to maize. Although SC was historically dominated by rice emissions, there are
 219 now areas where rice and maize exhibit comparable emission ratios to wheat.

220 In comparison to CO₂ emissions, the distribution of N₂O emission contributions displays more significant variations
 221 across SCB regions, particularly in the number of municipalities where rice dominates. In HHHP, both maize and wheat
 222 contribute significantly, with a gradual increase in maize-dominated areas and a shift from wheat-dominated to maize-
 223 dominated areas.

224 Regional disparities in the contribution of major grain to CO₂ and N₂O emissions were more pronounced in areas

225 where both dryland crops and rice were cultivated in larger proportions. In NEC and SCB, maize had a higher contribution
226 to N₂O emissions than to CO₂ emissions. Conversely, in MLYP, rice contributed more to CO₂ emissions than to N₂O
227 emissions. In QTP, wheat had a greater contribution to CO₂ emissions than to N₂O emissions. In other regions, wheat
228 played a larger role in CO₂ emissions than in N₂O emissions, with some regions showing nearly equal contributions for
229 both gases.

230 Regional disparities and substantial inter-annual variations are evident in the contribution of major grain to water
231 demand, as illustrated in Fig. 5b. In NEC and LP, maize stands out as the primary contributor to water demand, with an
232 increasing number of municipalities where maize is the main crop. In YGP, the historical dominance of rice is gradually
233 being supplanted by maize. Conversely, in SC, MLYP, and SCB, rice continues to dominate. HHHP exhibits the largest
234 proportion of areas dominated by maize and wheat, with a discernible upward trend. Notably, there's a gradual shift from
235 wheat-dominated to maize-dominated areas in HHHP.

236 Discussion

237 Efforts to optimize regional water allocations for a given water resource quantity are crucial for balancing regional
238 resources, ecological sustainability, and food security. Adapting cropping patterns to local climatic and soil conditions
239 can significantly alleviate water demand^{22,23}. Selecting drought-tolerant crops, for instance, not only minimizes irrigation
240 needs but also mitigates water wastage, curbing the overexploitation of groundwater and river water in agriculture²⁴. This
241 contributes to the sustainable management of water resources.

242 Simultaneously, aligning with the Chinese government's goals of reaching peak carbon emissions around 2030 and
243 achieving net-zero emissions by 2060²⁵, adjustments in cropping patterns can play a pivotal role in reducing GHG
244 emissions. Growing crops suited to local climatic conditions, particularly those adapted to mitigating methane emissions,
245 can effectively contribute to these emission reduction targets²⁶.

246 The study findings underscore significant variations in GHG emissions and water requirements among different
247 crops across diverse regions. Notably, the cultivation of single cropping rice generally exhibits higher GHG emission
248 intensity and water demand, aligning with broader research outcomes²⁷. Adjustments in cropping patterns, as
249 demonstrated in this study, can effectively realize agricultural water savings and emission reductions, thereby contributing
250 to the achievement of Sustainable Development Goals (SDGs). Inter-regional disparities are essential considerations for
251 tailoring targeted measures to refine water-saving and emission-reducing cropping patterns.

252 This research furnishes detailed crop emission and water demand maps grounded in actual regional production and

253 climatic soil conditions, leveraging highly specific crop data. Such information provides a foundational dataset for
254 informed cropping pattern adjustments and regional crop reallocation. For instance, strategically reducing the planting
255 area of single cropping rice and spring wheat in the Northeast region while increasing maize cultivation can significantly
256 diminish GHG emission intensity in the area. Similarly, augmenting the planting area of winter wheat and early rice in
257 MLYP, coupled with a reduction in single cropping rice cultivation, can mitigate carbon emissions. Given the substantial
258 water demand of single cropping rice in HHHP, prudent reductions in its cultivation can alleviate pressure on water
259 resources in the region. Clearly delineating spatial disparities in emissions and water requirements among different crops
260 will optimize the impact of judicious planting patterns.

261 The results of this study open avenues for further exploration of the interactions between cropping patterns and
262 various factors. Future research could delve into the impact of climate change on GHG emissions and water demand,
263 considering food cultivation patterns and farmland. Integration of ecosystem models and climate models could simulate
264 how cultivation patterns adapt to changing climate conditions. Additionally, understanding the influence of cropping
265 patterns on soil health and quality is vital for developing effective soil management strategies. Exploring biodiversity
266 dynamics under shifting cropping patterns and optimizing water resource conservation, encompassing changes in
267 irrigation demand and water quality, are essential considerations.

268 Furthermore, comprehensive assessments should include social impacts, policy frameworks, and institutional
269 orientations toward the sustainability of cropping patterns. Research on technological innovations resulting from shifts in
270 cropping patterns can provide valuable insights. This multifaceted approach can deepen our understanding of the
271 environmental impacts of cropping pattern shifts and contribute to the formulation of concrete policy and practice
272 recommendations for the development of sustainable agriculture.

273

274 **Materials and methods**

275 **Database and source**

276 The day-by-day meteorological data came from 377 meteorological stations in China (including maximum and
277 minimum temperatures and daily precipitation), and meteorological data sets were from the China Meteorological
278 Administration. Each city was assigned the nearest meteorological station based on the geometric center and the
279 distribution of meteorological stations is shown in Fig. S1. The CO₂ concentration background data used the average CO₂
280 data published by NOAA (<https://gml.noaa.gov/ccgg/>).

281 Soil data (including bulk, texture and clay content, organic matter and pH) were obtained from the Chinese soil
282 dataset (v1.1) based on the World Soil Database (HWSD). The data source within China was the 1:1 million soil data
283 provided by the Nanjing Soil Institute of the Second National Land Survey. The dataset covers all units at county level
284 and above; the dataset is quality controlled through strict manual auditing; the data format is grid raster format and the
285 projection is WGS84; the soil classification system used is mainly FAO-90. The dataset was provided by National
286 Cryosphere Desert Data Center. (<http://www.ncdc.ac.cn>).

287 Area, yield, fertilizer use and irrigated area for corn, wheat and rice at provincial-scale were from the China Statistical
288 Yearbook 1995-2020(<https://www.stats.gov.cn/tjsj>). Data on municipal-scale came from the China Agricultural Statistical
289 Yearbook, provincial statistical yearbooks, and regional statistical bulletins on national economic and social development
290 (Data source: <https://www.cnki.net/>).

291 As the statistics only contain the total amount of fertilizer used, we determined a quotient factor β for fertilizer
292 applied to each crop based on crop growth characteristics and relevant literature²⁸, and calculated the amount of fertilizer
293 used for each crop according to the following formula:

$$294 F_i = \frac{F_{sum}}{\sum A_i} \times \alpha \times \beta_i \quad (1)$$

295 Where F_i is the amount of fertilizer used for crop i ; F_{sum} is the total amount of fertilizer used for the three crops;
296 α is the total of the three crops as a proportion of the area sown to crops; A_i is the area planted to crop i ; β_i is the
297 fertilizer rationing factor for crop i .

298 Three fertilizer applications were set for each crop, in the ratio of 5:3:2²⁹. In this study, 15% of the straw was returned
299 to the field as organic fertilizer as there was no corresponding data on organic fertilizer use. Unlike the other two dryland

300 crops, flood irrigation for rice starts 7 days before transplanting and continues until a week before the harvest. Crop
301 planting and harvesting dates were summarised from ³⁰for the growth period of major grain in each province according
302 to the FAO handbook³¹, see Fig. S2.

303 **The DNDC model**

304 The DNDC model is a mechanistic model of the process based on nitrification and decomposition³². After years of
305 optimisation and adjustment, it is highly adaptable to a wide range of cropping systems in China, including corn, rice and
306 wheat. The GHG flux simulations have high accuracy and good performance³³⁻³⁵. The water demand module of the DNDC
307 model is based on the FAO-PM formula as well as the crop coefficient method for calculations, where the crop coefficients
308 of the model are fixed, but Crop coefficients are partly influenced by meteorological conditions³⁶. In this study, the crop
309 coefficients were modified according to the following equation::

$$310 \quad K_c = K_{cb} + [0.04(u_2 - 2) - 0.004(RH_{min} - 45)] \left(\frac{h}{3} \right)^{0.3} \quad (2)$$

311 Where K_{cb} are the K_c values reported in FAO 56 for the standard climate (i.e. mean $u_2 = 2.0$ m/s and mean
312 $RH_{min} = 45\%$), and recently updated by³⁷.; u_2 is the wind speed at a height of 2m during the crop growth stage(m/s);
313 RH_{min} is the minimum relative humidity at the crop growth stage(%); h is the average height of the crop(m).

314 The DNDC model mainly consists of a site-based meteorological database and 10 municipality-based stored soil and
315 farm management databases at the time of the run. A total of 1193 simulated units were included in this study, including
316 337 for corn, 238 for winter wheat, 102 for spring wheat, 260 for single cropping rice, and 128 each for early and late
317 rice.

318 In order to evaluate the influence of various GHGs on climate change, the global warming potential (GWP) spanning
319 100 years is used to express the combined warming effect of three GHGs³⁸. It is to assess the potential climate impact of
320 different GHGs based on their radiation properties. The calculation method is as follows:

$$321 \quad GWP = CO_2 + N_2O \times 273 + CH_4 \times 27 \quad (3)$$

322 Where GWP is global warming potential, kgC/ha; CO_2 is cumulative emission flux of CO_2 ; N_2O is cumulative
323 emission flux of N_2O ; CH_4 is cumulative emission flux of CH_4 ; 298 is the conversion factor of global warming
324 potential between N_2O and CO_2 ; 25 is the conversion factor of global warming potential between CH_4 and CO_2 .

325

326 **Model point validation data**

327 The model was validated using three parameters from published papers: GHG emissions, soil moisture and yield.
328 "Rice", "wheat", "corn", "DNDC", "Greenhouse gas" and "China" were used as keywords to obtain peer-reviewed
329 publications on the "Web of Science" website. The data from 29 sites across China were selected, and the detailed site
330 information is shown in Table. S2. Soil temperature, yield and GHG emission fluxes measured in the field experiment
331 were used to assess the applicability of the DNDC model in China. The following indices were used to evaluate the
332 performance of the model:

333 The root-mean-square error (RMSE) describes the deviation between the predicted and observed values in absolute
334 terms. The calculation is:

$$335 \quad RMSE = \sqrt{\frac{\sum_{i=1}^n (y_i - \hat{y}_i)^2}{n}} \quad 4)$$

336 R-squared (R^2) was used to measure the linear relationship between the observed and simulated values. It was
337 calculated as:

$$338 \quad R^2 = 1 - \frac{SSR}{SST} = 1 - \frac{\sum (y_i - \hat{y}_i)^2}{\sum (y_i - \bar{y})^2} \quad 5)$$

339 Where \hat{y}_i is the simulated value; y_i is the observed value; \bar{y} is the average of the observed value.

340 Uncertainty analysis

341 The uncertainty in the simulation results of this study focuses on three main aspects. Firstly, there was uncertainty
342 in the input data. Although all data input to the model was obtained from official Chinese statistics or statistics from world
343 authorities to ensure accuracy, there was still uncertainty in crop yields, climatic conditions, and soil properties. Soil
344 properties were particularly sensitive factors³⁹. In this study, the soil data used in the model is from the HWSD. However,
345 due to tillage, soil organic carbon content might continue to decline, leading to a possible overestimation of GHG
346 emissions.

347 Secondly, there is uncertainty in the model itself. Previous studies had shown that the model produces uncertainty in
348 simulation results under certain specific circumstances. For example, poorer simulation results for daily-scale N₂O fluxes
349 occurred when precipitation frequency and magnitude were high⁴⁰.

350 Finally, there was uncertainty in the model parameterization. In this study, the parameters were set based on previous
351 studies and expert knowledge. However, different parameter values could lead to different simulation results. Sensitivity
352 analysis of the model parameters could help identify the most critical parameters and their impacts on the simulation

353 results.

354 In summary, this study provided valuable insights into the regional differences in the contribution of major grain to
355 GHG emissions and water demand in China. However, the uncertainty in the simulation results needs to be considered
356 and addressed in future studies.

357

358 **Declarations of Competing interest**

359 The authors declare that they have no known competing financial interests or personal relationships that could have
360 appeared to influence the work reported in this paper.

361 **Acknowledgements**

362 This work was jointly supported by the National Natural Science Foundation of China (52122903, 51979230),
363 Science Fund for Distinguished Young Scholars of Shaanxi Province(2021JC20), Fok Ying-Tong Education Foundation
364 (171113) and Cyrus Tang Foundation, China National Postdoctoral Program for Innovative Talents (BX20220255).

365 **Contributions**

366 Yihe Tang analyzed the data and wrote the paper; Shikun Sun designed research; all authors reviewed the manuscript.

367 **Data availability**

368 Data will be made available on appropriate request.

369

370 **References**

- 371 1. Xie, W. *et al.* Crop switching can enhance environmental sustainability and farmer incomes in China. *Nature* **616**,
372 1–6 (2023).

373 2. Tubiello, F. N. *et al.* Pre- and post-production processes increasingly dominate greenhouse gas emissions from agri-
374 food systems. *Earth System Science Data* **14**, 1795–1809 (2022).

375 3. FAO. *FAOSTAT Emissions Totals*. <https://www.fao.org/faostat/en/#data/GT> (2021).

376 4. Postel, S., Vickers, A. & Starke, L. *Boosting Water Productivity*. (State of the World 2004, 2004).

377 5. Springmann, M. *et al.* Options for keeping the food system within environmental limits. *Nature* **562**, 519–525 (2018).

378 6. Cai, W. *et al.* Effects of mulching on water saving, yield increase and emission reduction for maize in China.
379 *Agricultural Water Management* **274**, 107954 (2022).

380 7. Tian, D. *et al.* The effect of drip irrigation and drip fertigation on N₂O and NO emissions, water saving and grain
381 yields in a maize field in the North China Plain. *Science of The Total Environment* **575**, 1034–1040 (2017).

382 8. Xu, H., Zhu, S. & Shi, H. Is It Possible to Reduce Agricultural Carbon Emissions through More Efficient Irrigation:
383 Empirical Evidence from China. *Water* **14**, 1218 (2022).

384 9. Bégué, A. *et al.* Remote Sensing and Cropping Practices: A Review. *Remote Sensing* **10**, 99 (2018).

385 10. Sun, S. K., Wu, P. T., Wang, Y. B. & Zhao, X. N. Impact of changing cropping pattern on the regional agricultural
386 water productivity. *The Journal of Agricultural Science* **153**, 767–778 (2015).

387 11. Huang, J. & Yang, G. Understanding recent challenges and new food policy in China. *Global Food Security* **12**, 119–
388 126 (2017).

389 12. Iizumi, T. & Ramankutty, N. How do weather and climate influence cropping area and intensity? *Global Food
390 Security* **4**, 46–50 (2015).

- 391 13. Salman, S. A. *et al.* Changes in Climatic Water Availability and Crop Water Demand for Iraq Region. *Sustainability*
392 **12**, 3437 (2020).
- 393 14. Tang, Y. *et al.* Impact assessment of climate change and human activities on GHG emissions and agricultural water
394 use. *Agricultural and Forest Meteorology* **296**, 108218 (2021).
- 395 15. Zhang, J. *et al.* Increased greenhouse gas emissions intensity of major croplands in China: Implications for food
396 security and climate change mitigation. *Global Change Biology* **26**, 6116–6133 (2020).
- 397 16. Yu, X., Keitel, C., Zhang, Y., Wangeci, A. N. & Dijkstra, F. A. Global meta-analysis of nitrogen fertilizer use
398 efficiency in rice, wheat and maize. *Agriculture, Ecosystems & Environment* **338**, 108089 (2022).
- 399 17. Foulkes, M. J. *et al.* Identifying traits to improve the nitrogen economy of wheat: Recent advances and future
400 prospects. *Field Crops Research* **114**, 329–342 (2009).
- 401 18. Carlson, K. M. *et al.* Greenhouse gas emissions intensity of global croplands. *Nature Clim Change* **7**, 63–68 (2017).
- 402 19. Snyder, C. S., Bruulsema, T. W., Jensen, T. L. & Fixen, P. E. Review of greenhouse gas emissions from crop
403 production systems and fertilizer management effects. *Agriculture, Ecosystems & Environment* **133**, 247–266 (2009).
- 404 20. Anapalli, S. S. *et al.* Quantifying water and CO₂ fluxes and water use efficiencies across irrigated C₃ and C₄ crops
405 in a humid climate. *Science of The Total Environment* **663**, 338–350 (2019).
- 406 21. Liu, Y. *et al.* Spatio-temporal variation of irrigation water requirements for wheat and maize in the Yellow River
407 Basin, China, 1974–2017. *Agricultural Water Management* **262**, 107451 (2022).
- 408 22. Davis, K. F., Rulli, M. C., Seveso, A. & D'Odorico, P. Increased food production and reduced water use through
409 optimized crop distribution. *Nature Geosci* **10**, 919–924 (2017).
- 410 23. Green, T. R., Yu, Q., Ma, L. & Wang, T.-D. Crop water use efficiency at multiple scales. *Agricultural Water
411 Management* **97**, 1099–1101 (2010).

- 412 24. Grogan, D. S. *et al.* Quantifying the link between crop production and mined groundwater irrigation in China. *Science of The Total Environment* **511**, 161–175 (2015).
- 413 25. Wei, Y.-M. *et al.* Policy and Management of Carbon Peaking and Carbon Neutrality: A Literature Review. *Engineering* **14**, 52–63 (2022).
- 414 26. He, L. *et al.* Optimal crop planting pattern can be harmful to reach carbon neutrality: Evidence from food-energy-water-carbon nexus perspective. *Applied Energy* **308**, 118364 (2022).
- 415 27. Wang, X. *et al.* Global irrigation contribution to wheat and maize yield. *Nat Commun* **12**, 1235 (2021).
- 416 28. ZPDARA. *Comments on the trial of a fixed-rate system for agricultural inputs of fertilizers*. http://www.zjagri.gov.cn/art/2019/8/7/art_1589297_36435903.html (2019).
- 417 29. Wang, Z. *et al.* Inhibition of methane emissions from Chinese rice fields by nitrogen deposition based on the DNDC model. *Agricultural Systems* **184**, 102919 (2020).
- 418 30. Zheng, Y. Research on the Spatial-temporal distribution of growth period of main grain crops and its change in China. (Central China Normal University, 2015).
- 419 31. Allen, R. *et al.* Crop Evapotranspiration: Guidelines for Computing Crop Water Requirements, FAO Irrigation and Drainage Paper 56. *FAO* **56**, (1998).
- 420 32. Li, C., Frolking, S. & Frolking, T. A. A model of nitrous oxide evolution from soil driven by rainfall events: 1. Model structure and sensitivity. *Journal of Geophysical Research: Atmospheres* **97**, 9759–9776 (1992).
- 421 33. Li, H. *et al.* The development of China-DNDC and review of its applications for sustaining Chinese agriculture. *Ecological Modelling* **348**, 1–13 (2017).
- 422 34. Liu, Z. *et al.* Impacts of mulching measures on crop production and soil organic carbon storage in a rainfed farmland area under future climate. *Field Crops Research* **273**, (2021).

- 433 35. Yu, C. *et al.* Managing nitrogen to restore water quality in China. *Nature* **567**, 516–520 (2019).
- 434 36. Allen, R. G. & Pereira, L. S. Estimating crop coefficients from fraction of ground cover and height. *Irrig Sci* **28**, 17–
- 435 34 (2009).
- 436 37. Pereira, L. S. *et al.* Standard single and basal crop coefficients for vegetable crops, an update of FAO56 crop water
- 437 requirements approach. *Agricultural Water Management* **243**, 106196 (2021).
- 438 38. IPCC. *Climate Change 2021: The Physical Science Basis*. <https://www.ipcc.ch/report/ar6/wg1/> (2021).
- 439 39. Zhang, F., Qi, J., Li, F. M., Li, C. S. & Li, C. B. Quantifying nitrous oxide emissions from Chinese grasslands with
- 440 a process-based model. *Biogeosciences* **7**, 2039–2050 (2010).
- 441 40. Foltz, M. E., Zilles, J. L. & Koloutsou-Vakakis, S. Prediction of N₂O emissions under different field management
- 442 practices and climate conditions. *Sci Total Environ* **646**, 872–879 (2019).
- 443

1 **Supplementary Information for:**
2 **Cropping pattern switching induces disturbances in spatiotemporal greenhouse gas emissions and**
3 **water demand**

4 **Supplementary Results**

5 **DNDC model validation and parameterization**

6 The DNDC model has undergone validation using field experimental data from the literature. This
7 study utilized 31 sets of field data from peer-reviewed publications to assess the feasibility of the DNDC
8 model in mainland China, with the dataset representative of different agricultural regions across the
9 country. Specific site information can be found in Table S4. The RMSEs for soil temperature, daily
10 emission fluxes of CO₂, CH₄, and N₂O fell within the intervals 0.1-4.2°C, 12.9-42kgC/ha·d, 0.01-
11 2.31kgC/ha·d and 0.02-2.59 kgN/ha·d, respectively. The consistency of the day-to-day fluctuation trends
12 and peaks between the simulated and measured data (Fig. S12a-h) demonstrated that the model can
13 simulate a wide range of croplands across China with promising results. The parameterised model crop
14 parameter ranges are shown in Table S3.

15 After confirming the feasibility of the DNDC model in simulating major grain crops in China, the
16 model was run with cities as the basic simulation unit. There were notable differences between the
17 simulated yields and measured values due to crop varieties and regional adaptations of crops. We selected
18 parameters such as maximum biomass, the biomass ratio of the grain, thermal degree days (TDD), water
19 requirement, and growth period, and used the Monte Carlo method to match the DNDC model with
20 regional parameters.

21 We simulated 1191 samples for six crops, with yield as the validation item (Fig. S12i). Following
22 parameterization, the model simulations aligned well with the majority of the areas in China. Simulated
23 and observed yields were fitted with R² of 0.96 (n=1191), with RMSE of 158 kg/ha. Simulated yields for
24 each crop were also well-fitted, with R² of 0.94 (n=329) for corn, R² of 0.90 (n=249) for winter wheat,
25 R² of 0.95 (n=102) for spring wheat, R² of 0.90 (n=259) for single cropping rice, R² of 0.92 (n=126) for
26 early rice, and R² of 0.90 (n=259) for late rice. We developed a set of parameters to match the actual
27 ecological conditions of Chinese farmland, and the model simulation allows for a more precise estimation

28 of greenhouse gas emissions of major crops in China.

29 **Spatial and temporal evolution of cropping patterns**

30 The cultivation scale of China's grain has exhibited a fluctuating upward trend, with four distinct
31 stages of change (Fig. 1b). Initially, from 1995 to 1998, there was a continuous rise, during which the
32 acreage of staple grain increased from 84.37 Mha to 88.22 Mha, marking a 4.56% increase. The following
33 period, from 1998 to 2003, witnessed a decline in acreage, reaching the lowest value of 74.58 Mha.
34 However, from 2003 to 2015, there was a steady increase in acreage for 12 years, culminating in the
35 highest-ever recorded acreage of staple grain at 102.33 Mha. After 2015, the grain acreage saw a decline
36 once again to 96.73 Mha. In terms of crop type, the area of corn demonstrated the most significant upward
37 trend, exhibiting an increase of 97.44%. Except for corn and single cropping rice, which displayed an
38 overall upward trend during the study period, the acreage of the other four grains declined to varying
39 degrees. Of these, spring wheat showed the largest decrease, with a decline of 217.50%.

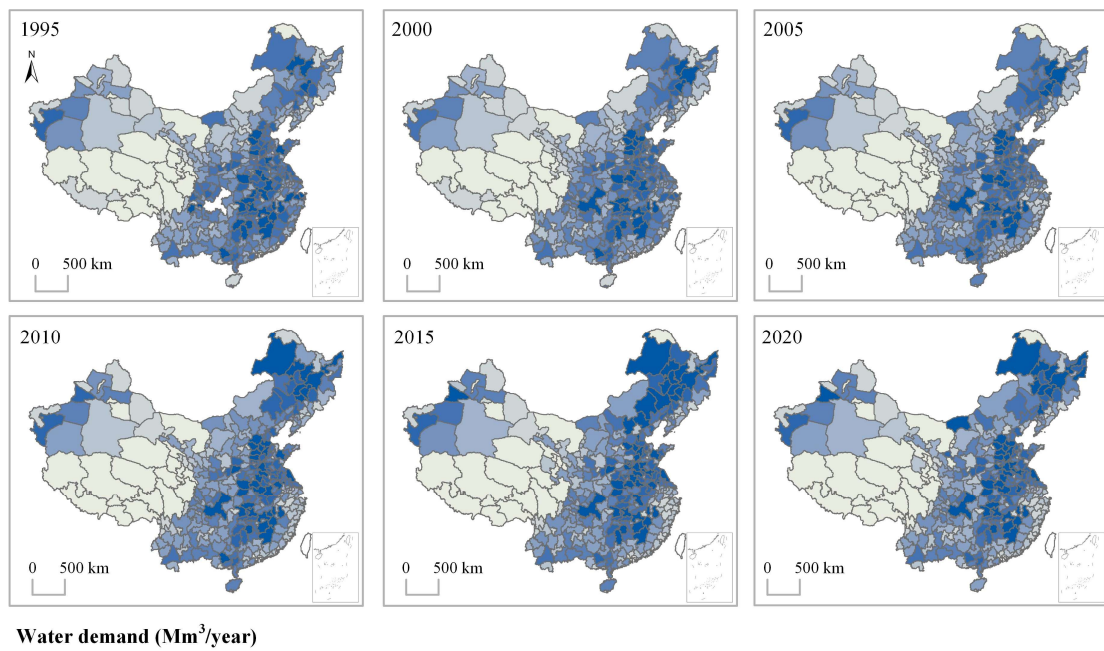
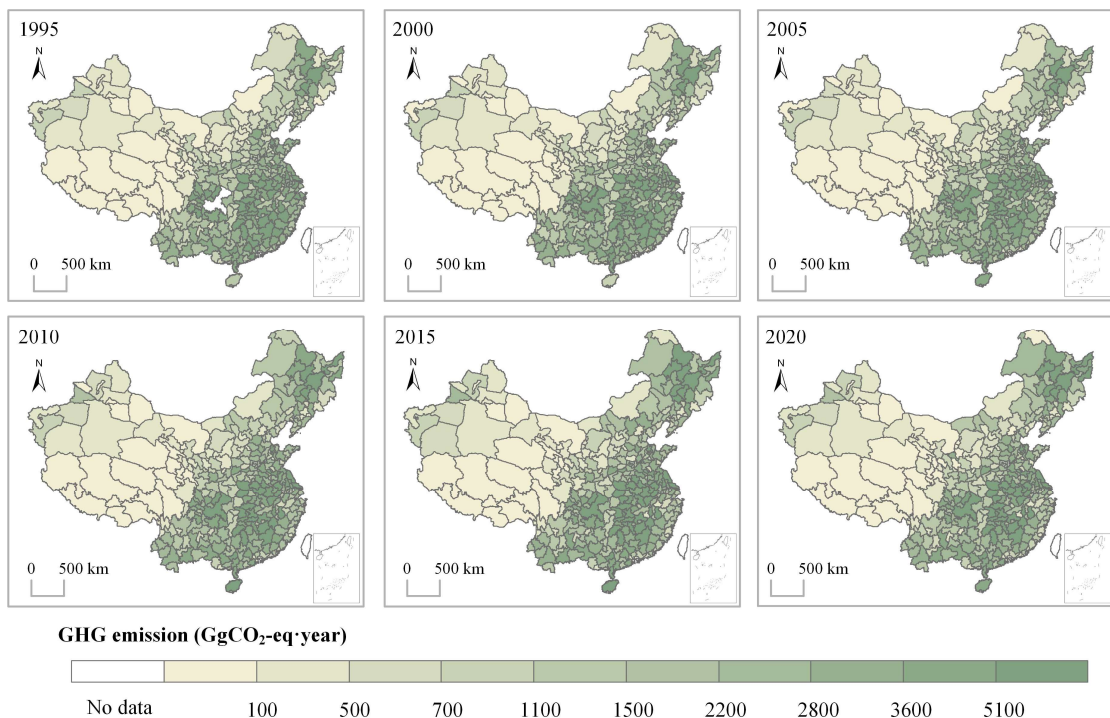
40 The trends in acreage for each agricultural region varied over the study period Fig. S4a. The
41 Northeast China Plain (NEC) demonstrated a continual increase in the area planted to corn between 2000
42 and 2015, overtaking the Huang-Huai-Hai Plain (HHHP) as the largest corn-growing region in 2010. The
43 HHHP is the major spring wheat growing region followed by the Middle-lower Yangtze Plain (MLYP)
44 and these two regions account for more than 75.69% of the total area. The acreage of spring wheat
45 reached its lowest value in 2005, but after that, there was a gradual increase in the acreage of spring
46 wheat in China. This increase was driven by the HHHP, the MLYP, and the Northern arid and semiarid
47 region (NASR). The acreage of winter wheat in China demonstrated a continuous decline since 1995,
48 particularly in the two primary winter wheat growing regions, the NEC and the NASR. In both regions,
49 the reduction in acreage reached 50%. The expansion of single cropping rice acreage was augmented by
50 increases in single cropping rice acreage in the NEC and the MLYP, with these two regions accounting
51 for more than 90% of the total increase nationwide. The acreage of early and late rice continued to decline
52 within each region during the study period and exhibited the same trend of change. The trend of change
53 was most pronounced in the MLYP, where there was a 33.67% decline.

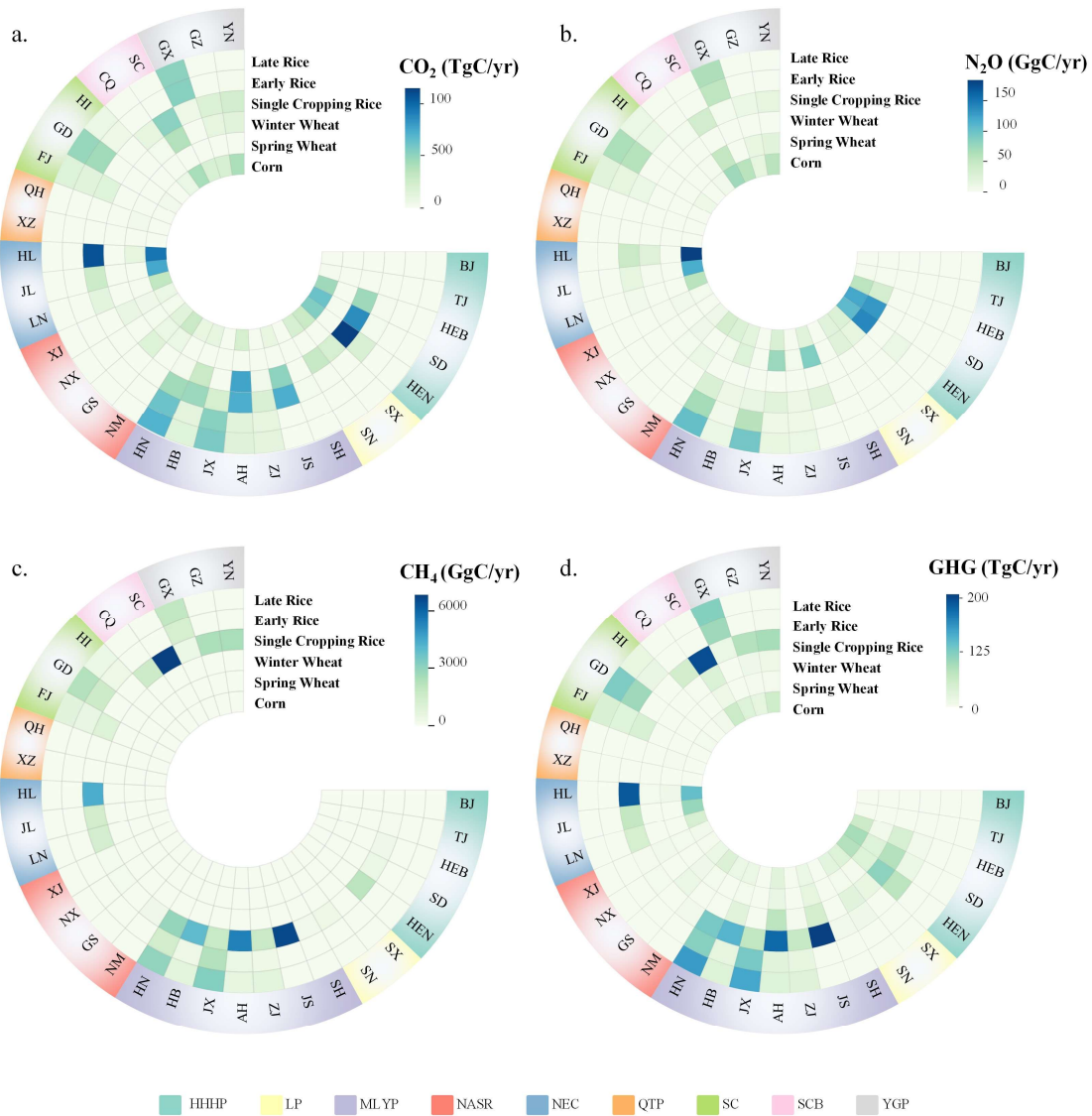
54 Disregarding the varietal subcategories of grain, we can observe temporal and spatial changes in the
55 proportions of corn, rice, and wheat, the three main grains, across various municipal administrative

56 regions during the study period. As shown in Fig. 1a, since 1995, in northern China (including Northeast
57 and Northwest), cities where wheat was the dominant crop (with the planting area >50%) have gradually
58 been replaced by corn and rice. The number of cities where corn was the dominant crop increased from
59 53 in 1995 to 133 in 2020, representing a growth of 150.94%. This had replaced most of the provinces
60 where wheat was the predominant crop. Rice, due to its specific planting conditions, has maintained a
61 high level of dominance in the number of cities with no significant spatial and temporal trends. There
62 were significant differences in the dominant crops in various agricultural regions. Cities dominated by
63 wheat were mainly concentrated in the northwest and central regions of China, while areas where corn
64 dominates are mainly in the northeast, north, and southwest regions of China, with a trend of expanding
65 towards the northwest and central regions. The areas where rice dominates are mainly concentrated in
66 the southeast and northwest regions, with the southwest region mainly consisting of double-season rice
67 and other regions consisting of single cropping rice.

68

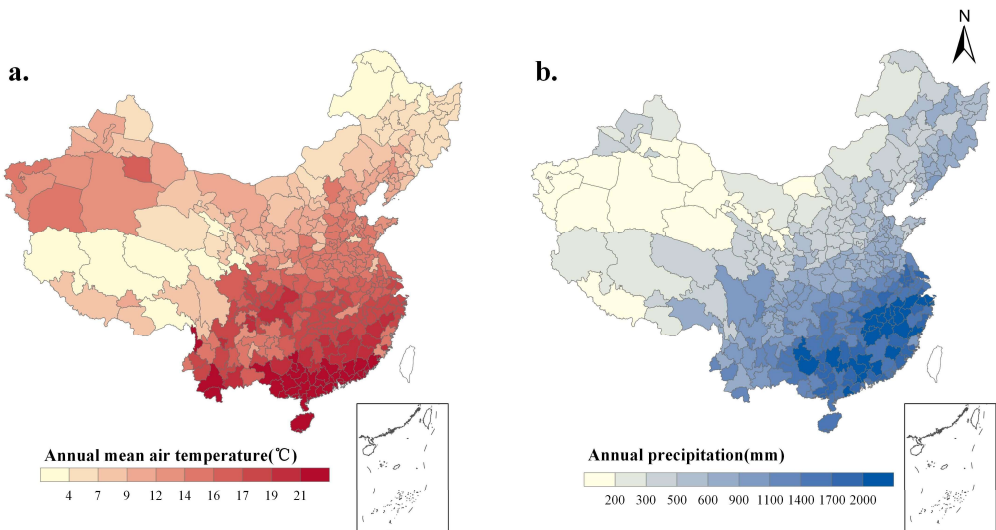
69 **Supplementary Information Figures**





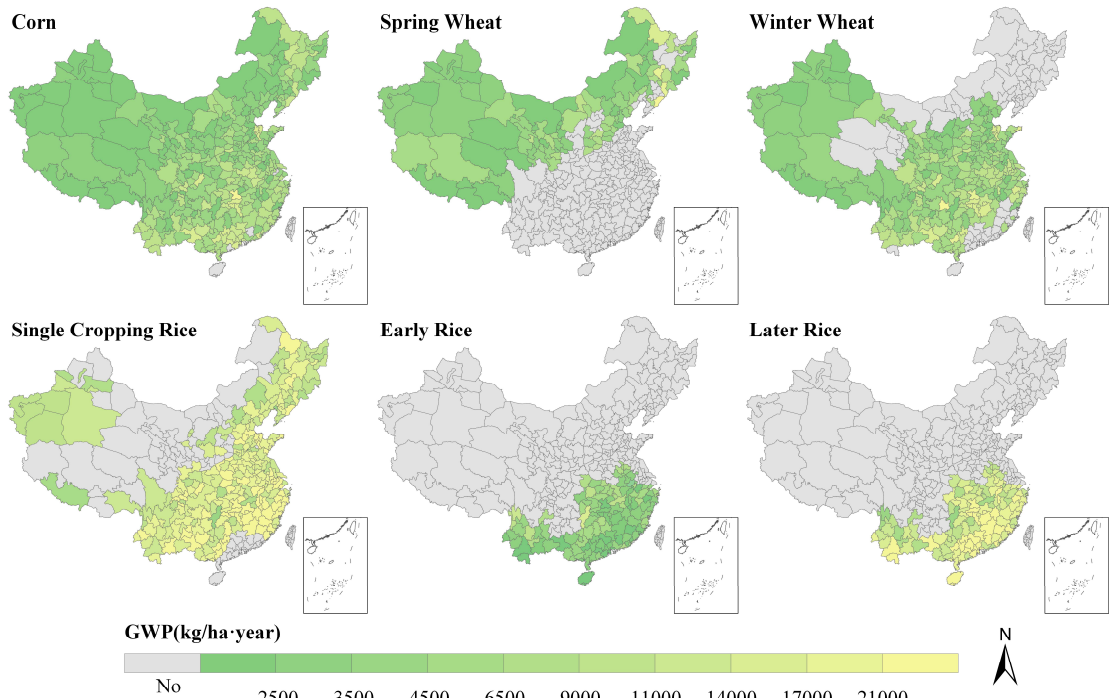
77
78
79

Fig. S3 Heat map of annual average emission of each crop for three ghgs by province. (Take 2015 for example)



80
81

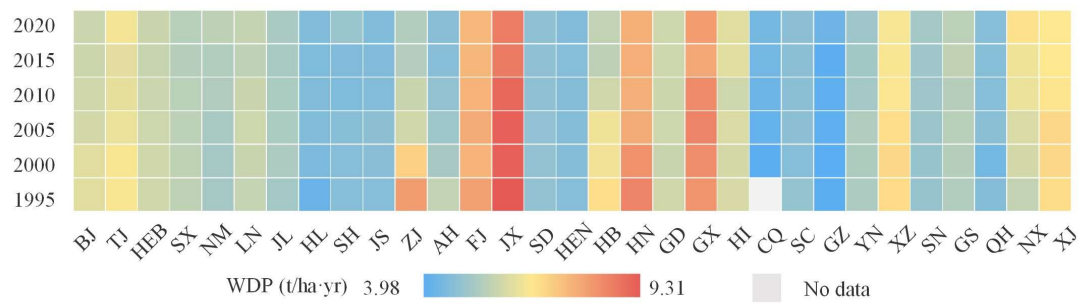
Fig. S4 Annual precipitation and average temperature



82

83

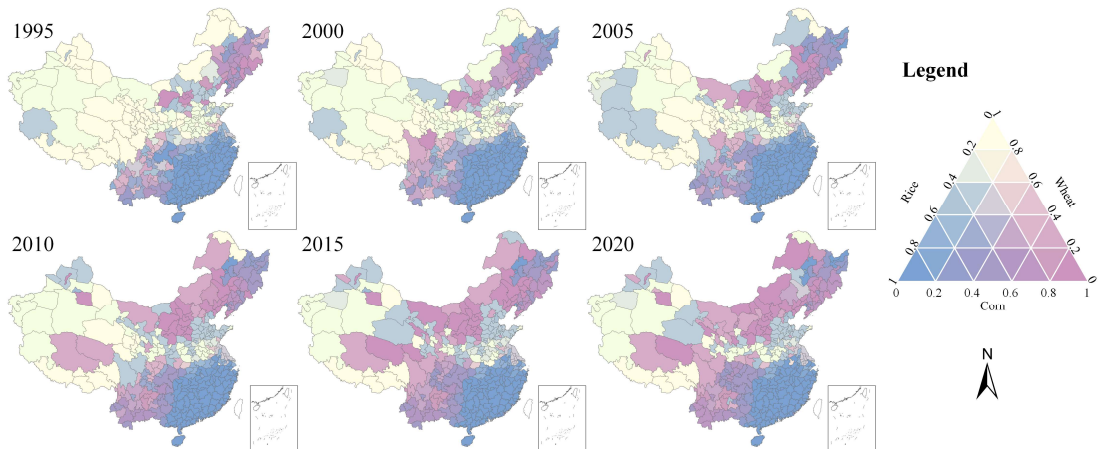
Fig. S1 Municipal-scale greenhouse gas emission intensity in China



84

85

Fig. S6 Water demand per unit area for major grain in China's provinces from 1995 to 2020



86

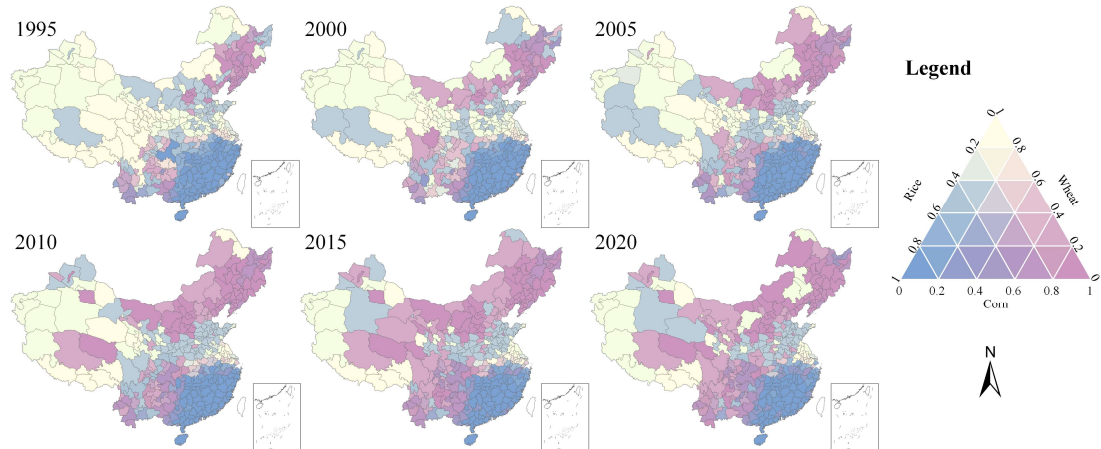
87

Fig. S7 Contribution of major grain to CO₂ emissions. (The legend is a ternary graph showing the contribution of each crop to the emissions in the region, the closer the colour to blue the greater the contribution of rice, the closer the colour to yellow the greater the contribution of wheat and the closer the colour to pink the greater the contribution of corn.)

88

89

90

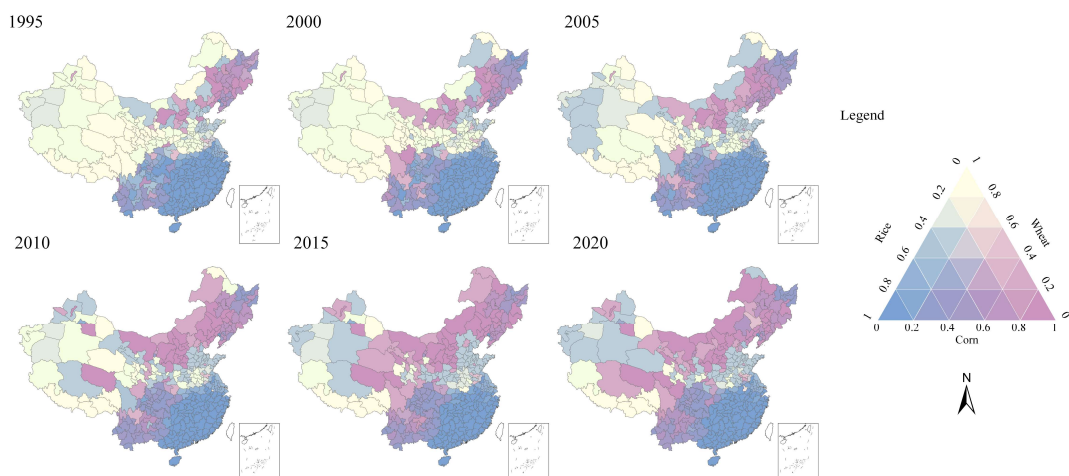


91

92 Fig. S8 Contribution of major grain to N₂O emissions. (The legend is a ternary graph showing the
 93 contribution of each crop to the emissions in the region, the closer the colour to blue the greater the
 94 contribution of rice, the closer the colour to yellow the greater the contribution of wheat and the closer
 95 the colour to pink the greater the contribution of corn.)

96

97

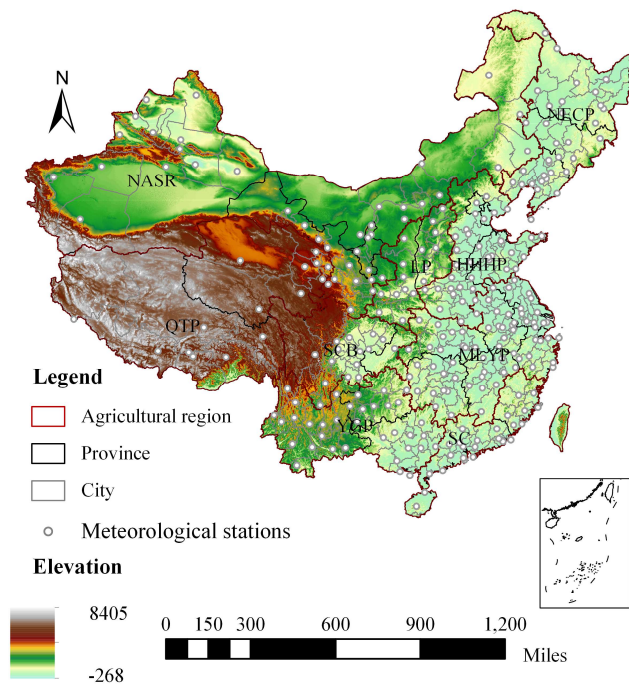


98

99 Fig. S9 Contribution of major grain to water demand. (The legend is a ternary graph showing the
 100 contribution of each crop to the emissions in the region, the closer the colour to blue the greater the
 101 contribution of rice, the closer the colour to yellow the greater the contribution of wheat and the closer
 102 the colour to pink the greater the contribution of corn.)

103

104



105

106 Fig. S10 Overview of the study area (The map includes the division of each municipality, province and
 107 agricultural region as well as the distribution of meteorological stations. For further information
 108 regarding the specific division of regions, provinces, and municipalities, readers are referred to Table
 109 S1)

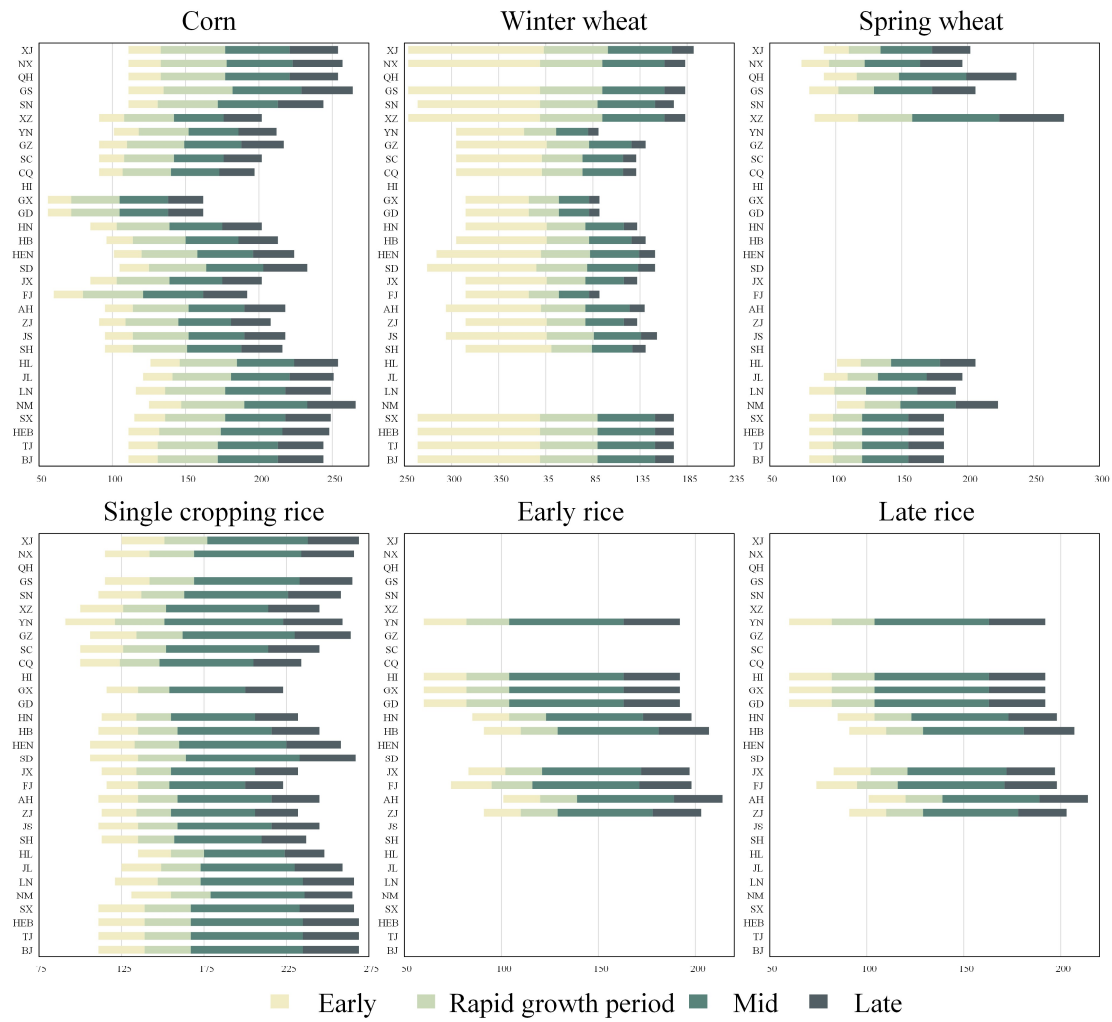
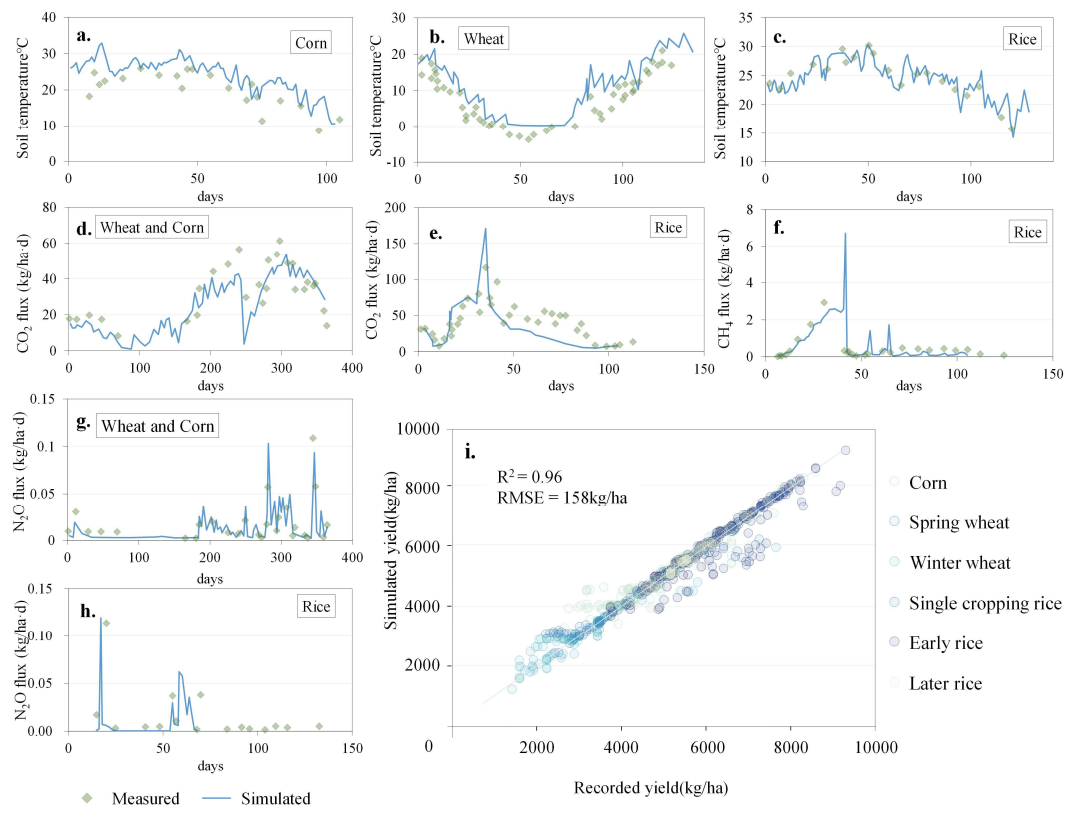


Fig. S11 Provincial crop growth period(The abscissa is day of year)



112

113

Fig. S12 Simulated and measured soil temperature (a to c), daily CO_2 flux (d to e), daily CH_4 flux (f),
daily N_2O flux (g to h) and yield(i).

114

115

116 **Supplementary Information tables**

117 Table S1 Agricultural regional division and abbreviations of provincial administrative regions

Agricultural region		Province	
Northeast China Plain	NEC	Liaoning	LN
		Jilin	JL
		Heilongjiang	HL
Yunnan-Guizhou Plateau	YGP	Guizhou	GZ
		Yunnan	YN
		Guangxi	GX
Northern arid and semiarid region	NASR	Gansu	GS
		Ningxia	NX
		Xinjiang	XJ
		NeiMengGu	NM
Southern China	SC	Guangdong	GD
		Hainan	HI
		Fujian	FJ
Sichuan Basin and surrounding regions	SCB	Chongqing	CQ
		Sichuan	SC
Middle-lower Yangtze Plain	MLYP	Hebei	HB
		Hunan	HN
		Jiangxi	JX
		Shanghai	SH
		Jiangsu	JS
Qinghai Tibet Plateau	QTP	Zhejiang	ZJ
		Anhui	AH
		Xizang	XZ
		Qinghai	QH
Loess Plateau	LP	Shaanxi	SN
		Shanxi	SX
Huang-Huai-Hai Plain	HHHP	Beijing	BJ
		Tianjin	TJ
		Hebei	HEB
		Henan	HEN
		Shandong	SD

118

119

120

Table S2 Input parameters required for regional simulation with DNDC

Items	Input parameters
Climate	Temperature, precipitation, rainfall N concentration
Soil	SOC, soil texture, pH, bulk density
Crop parameters	Acreage, maximum yield, thermal degree days, water demand, growing degree days
Management	Planting date, harvest date, fertilizer application rate, film mulch, manure amendment, tillage, residue incorporation

121

122

Table S3 Parameterized range of major crop parameters

Crop	Variables	Database
Corn	Max grain yield (kgC/ha)	2000-5000
	Ratio of grain organs	0.25-0.4
	TDD (°C)	1800-2100
Wheat	Max grain yield (kgC/ha)	500-2500
	Ratio of grain organs	0.25-0.45
	TDD (°C)	1600-1900
Rice	Max grain yield (kgC/ha)	2000-5000
	Ratio of grain organs	0.2-0.4
	TDD (°C)	1900-2200

123

Note: Crop parameters for winter and spring wheat varied across simulation units, although the range of variation remained consistent. Similarly, this held true for early, late, and single cropping rice.

124

125

126

Table S4 Basic information on validation points

Crop	Province	longitude and latitude	pH	Bulk density (g·cm ⁻³)	clay	SOC (g·kg ⁻¹)	year	References
Corn	Cangzhou, Hebei	37°63'N, 116°44'E	7.4	1.68	0.11	12.7	2019-2020	(Wang et al., 2022)
Corn	Quzhou, Hebei	36°52'N, 115°01'E	7.72	1.37		12.6	2009-2013	(Abdalla et al., 2022)
Corn	Quzhou, Hebei	36°31'N, 115°00'E	7.97	1.38	/	8.5	2006-2006	(Li et al., 2010)
Corn	Quzhou, Hebei	36°52'N, 115°01'E	8.3	1.36	/	14.2	2012	(Abdalla et al., 2020; Song et al., 2018)
Corn	Dalian, Liaoning	39°30'N, 121°45'E	7.6	1.38		12.3	2009	(Li et al., 2012)
Corn	Yangling, Shanxi	34°17'N, 108°00'E	8.6	1.34	0.32	15.1	2015-2016	(Lv et al., 2020)
Corn	Yangling, Shanxi	34°20'N, 108°24'E	8.2	1.37	0.17	8.14	2013-2016	(Chen et al., 2019)
Corn	Yongji, Shanxi	34°55'N, 110°42'E	8.7	1.17	0.32	11.3	2007-2010	(Zhang et al., 2015)
Corn	Yongji, Shanxi	36°58'N, 117°59'E	8.3	1.42	0.17	1.05	2008-2010	(Zhang et al., 2015)
Corn	Yongji, Shanxi	36°58'N, 117°59'E	8.3	1.32	0.19	8.5	2004-2007	(Zhang et al., 2015)
Corn	Tingzhou, Beijing	39°41'N, 116°41'E	7.8	1.57	0.32	11.06	2013-2015	(Chi et al., 2020)
Corn	Cangzhou, Hebei	37°63'N, 116°44'E	7.4	1.68	0.11	12.7	2018-2020	(Wang et al., 2022)
Wheat	Cangzhou, Hebei	37°63'N, 116°44'E	7.4	1.68	0.11	12.7	2018-2020	(Wang et al., 2022)
Wheat	Changshu, Jiangsu	31°32'N, 120°41'E	7.7	1.2	/	20.1	2012-2014	(Xia et al., 2016)
Wheat	Quzhou, Hebei	36°52'N, 115°01'E	7.72	1.37		12.6	2009-2013	(Abdalla et al., 2022)
Wheat	Quzhou, Hebei	36°31'N, 115°00'E	7.97	1.38	/	8.5	2005-2006	(Li et al., 2010)
Wheat	Quzhou, Hebei	36°52'N, 115°01'E	8.3	1.36	/	14.2	2012-2013	(Abdalla et al., 2020; Song et al., 2018)

Wheat	Yangling, Shanxi	34°17'N, 108°00'E	8.6	1.34	0.32	15.1	2015-2016	(Lv et al., 2020)
Wheat	Yangling, Shanxi	34°20'N, 108°24'E	8.2	1.37	0.17	8.14	2013-2016	(Chen et al., 2019)
Wheat	Yongji, Shanxi	34°55'N, 110°42'E	8.7	1.17	0.32	11.3	2007-2010	(Zhang et al., 2015)
Wheat	Yongji, Shanxi	36°58'N, 117°59'E	8.3	1.42	0.17	1.05	2008-2010	(Zhang et al., 2015)
Wheat	Yongji, Shanxi	36°58'N, 117°59'E	8.3	1.32	0.19	8.5	2004-2007	(Zhang et al., 2015)
Rice	Jian, Jiangxi	26°44'N, 115°04'E	5.00	1.31	0.14	10.0	2012-2014	(Sun et al., 2023)
Rice	Nanjing, Jiangsu	32°14'N, 118°42'E	6.57	1.36	0.26	25.0	2015-2016	(Chen et al., 2020)
Rice	Jiamusi, Heilongjiang	47°35'N, 133°31'E	5.61	0.98	0.41	27.7	2004	(Zhang et al., 2011)
Rice	Huaiyuan, Anhui	33°04'N, 117°05'E	7.5	1.45	0.19	16.0	2011-2012	(Zhang et al., 2022)
Rice	Shanghai	30°53'N, 121°23'E	7.6	1.40	0.27	13.7	2013-2016	(Zhang et al., 2019)
Rice	Suihua, Heilongjiang	46°57'N, 127°40'E	6.4	1.26	0.21	41.8	2017	(Nie et al., 2019)
Rice	Changshu, Jiangsu	31°32'N, 120°41'E	7.7	1.2	/	20.1	2013-2015	(Xia et al., 2016)
Rice	Kunshan, Jiangsu	34°63'N, 121°05'E	7.4	1.53	0.89	30.3	2003-2005	(Wu and Zhang, 2014)
Rice	Shanghai	30°53'N, 121°23'E	7.6	1.4	/	13.7	2013-2014	(Sun et al., 2016)